Electronic Supplementary Material (ESI) for Journal of Materials Chemistry C.
This journal is © The Royal Society of Chemistry 2016

Characterization of a P-Type Photomechanical Molecular Crystal Based on the E→Z Photoisomerization of 9-Divinylanthracene Malonitrile

Lingyan Zhu[(1)], Fei Tong[(1)], Norhan Zaghloul[(2)], Omar Baz[(2)], Christopher J. Bardeen[(1)]*, Rabih O. Al-Kaysi[(2)*],

[(1)] Department of Chemistry
University of California, Riverside
501 Big Springs Road
Riverside, CA 92521 (USA)

[(2)] College of Science and Health Professions-3124,
King Saud bin Abdulaziz University for Health Sciences, and King Abdullah International Medical Research Center, Ministry of National Guard Health Affairs, Riyadh 11426,
(Kingdom of Saudi Arabia)

*E-mail: kaysir@ksau-hs.edu.sa, rabihalkaysi@gmail.com
christopher.bardeen@ucr.edu

Figure S1. IR spectrum of (E)-9DVAM over KBr

Figure S2. ^{1}H-NMR of (E)-9DVAM in $CDCl_3$

Figure S3. IR spectrum of (Z)-9DVAM over KBr

Figure S4. ^{1}H-NMR of (Z)-9DVAM with 5% E-9DVAM isomer in $CDCl_3$

Table S1. Crystal data and structure refinement for (E)-9DVAM, and conditions to prepare single crystal

Figure S5. UV-Vis spectra of (E)-9DVAM in different solvents, color = solvent

Figure S6. The absorption spectra of (E)-9DVAM in THF

Figure S7. Fluorescence lifetime data and the corresponding emission spectra of (E)-9DVAM in different wavelength ranges

Figure S8. UV-Vis absorption spectra of (E)-9DVAM as a solid-state crystalline thin film and in solution with THF as the solvent

Figure S9. UV-Vis absorption spectra of (Z)-9DVAM as a solid-state crystalline thin film and in solution with THF as the solvent

Figure S10. HPLC analysis of (E)-9DVAM photoproducts after photolysis in solution

Figure S11. HPLC analysis of photoproducts from photolysis of crystalline (E)-9DVAM

Figure S12. Optical microscopy images of (E)-9DVAM microribbon actuating between UV (365 nm) and visible light (535 nm)

Figure S13. Optical microscopy images of (E)-9DVAM microcrystals actuating between UV (365 nm) and visible light (535 nm)

Figure S14. Powder X-ray diffraction patterns of (E)-9DVAM nanorods

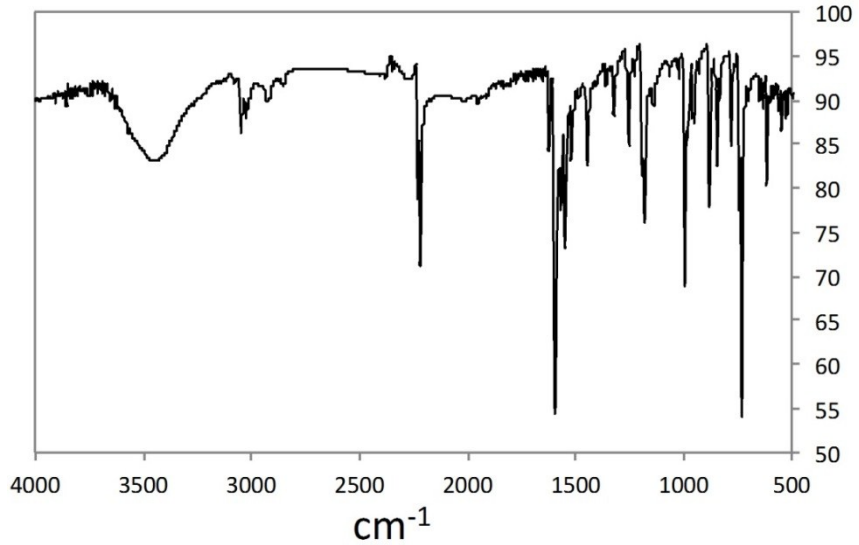

Figure S1. IR spectrum of (E)-9DVAM over KBr

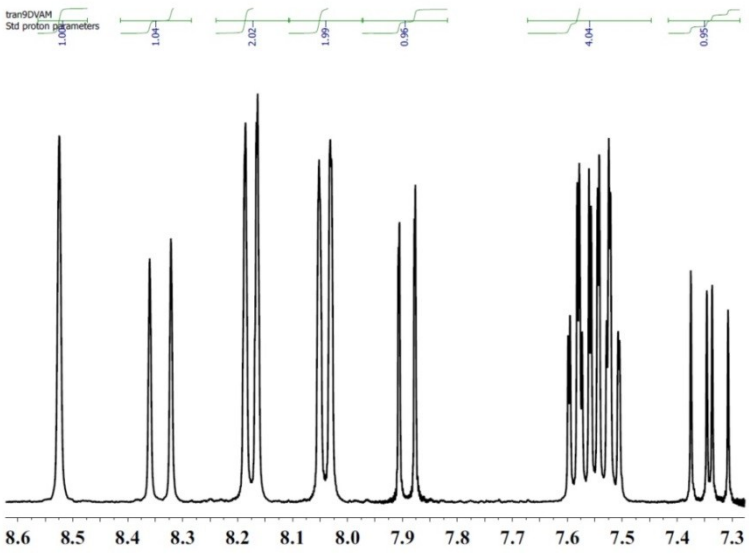

Figure S2. H-NMR of (E)-9DVAM in $CDCl_3$ δ (ppm): 7.30-7.48 (dd, 1H), 7.50-7.69 (m, 4H), 7.87-7.91 (d,1H), 8.03-8.05 (d, 2H), 8.16-8.19 (d, 2H), 8.32-8.36 (d, 1H), 8.52 (s 1H)

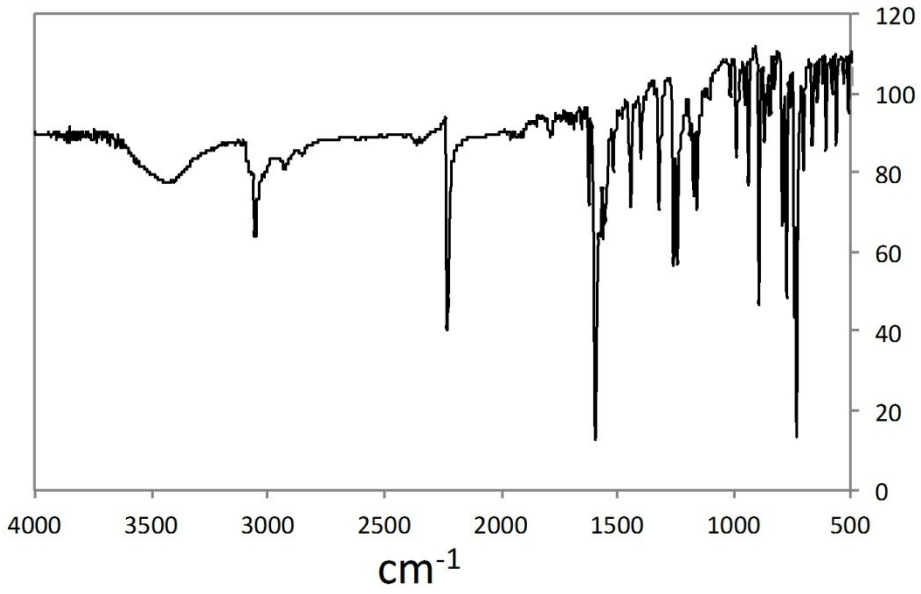

Figure S3. IR spectrum of (Z)-9DVAM over KBr

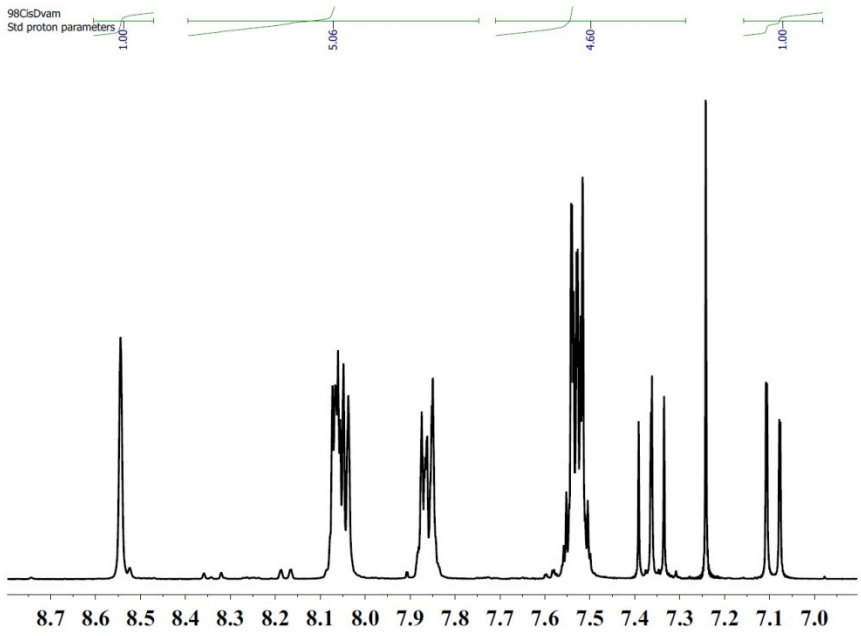

Figure S4. H-NMR of (Z)-9DVAM with 5% E-9DVAM isomer in $CDCl_3$ δ (ppm): 7.07-7.15 (d, 1H), 7.35-7.39 (t, H), 7.50-7.55 (m, 5H), 7.85-7.89 (m, 2H), 8.04-8.09 (m, 2H), 8.55 (s, 1H)

Table S1. Crystal data and structure refinement for (E)-9DVAM

Empirical formula	$C_{20}H_{12}N_2$	
Formula weight	280.32	
Temperature	100(2) K	
Wavelength	0.71073 Å	
Crystal system	Monoclinic	
Space group	P 21/n (#14)	
Unit cell dimensions	a = 19.293(3) Å	α= 90°.
	b = 4.0674(7) Å	β= 118.107(3)°.
	c = 20.370(4) Å	γ = 90°.
Volume	1410.0(4) $Å^3$	
Z	4	
Density (calculated)	1.321 Mg/m^3	
Absorption coefficient	0.078 mm^{-1}	
F(000)	584	
Crystal size	0.587 x 0.072 x 0.010 mm^3	
Theta range for data collection	1.999 to 25.342°.	
Index ranges	-23<=h<=23, -4<=k<=4, -24<=l<=24	
Reflections collected	23666	
Independent reflections	2577 [R(int) = 0.0795]	
Completeness to theta = 25.242°	99.9 %	
Absorption correction	Semi-empirical from equivalents	
Refinement method	Full-matrix least-squares on F^2	
Data / restraints / parameters	2577 / 0 / 199	
Goodness-of-fit on F^2	1.024	
Final R indices [I>2sigma(I)]	R1 = 0.0519, wR2 = 0.1248	
R indices (all data)	R1 = 0.0809, wR2 = 0.1413	
Extinction coefficient	n/a	
Largest diff. peak and hole	0.243 and -0.218 $e.Å^{-3}$	

Crystal Growth Conditions

To grow large single crystals for x-ray structure determination, (E)-DVAM (5 mg) was spread inside a small aluminum weighing pan and placed inside a vacuum drying vessel. A 1 cm diameter glass cylinder was placed surrounding the (E)-9DVAM powder. The vessel was heated to 200 ^oC under reduced pressure (20 mbar). The (E)-9DVAM quickly sublimes and deposits on the surface of the glass cylinders as large X-ray quality crystals. A sample of these sublimed crystals was analyzed by HPLC to confirm purity and that no decomposition had taken place.

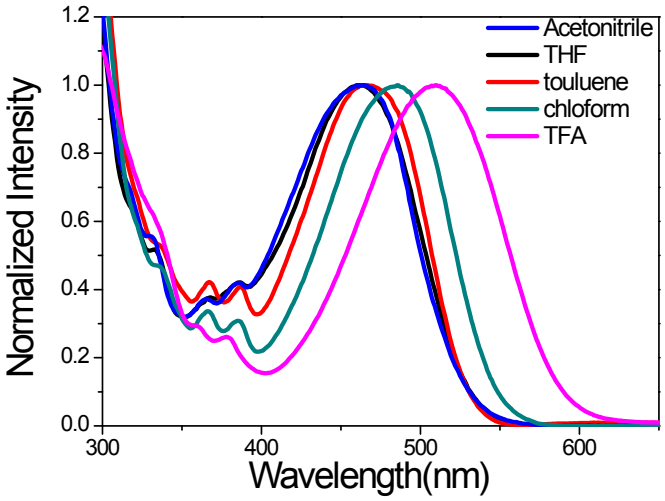

Figure S5. UV-Vis spectra of (E)-9DVAM in different solvents.

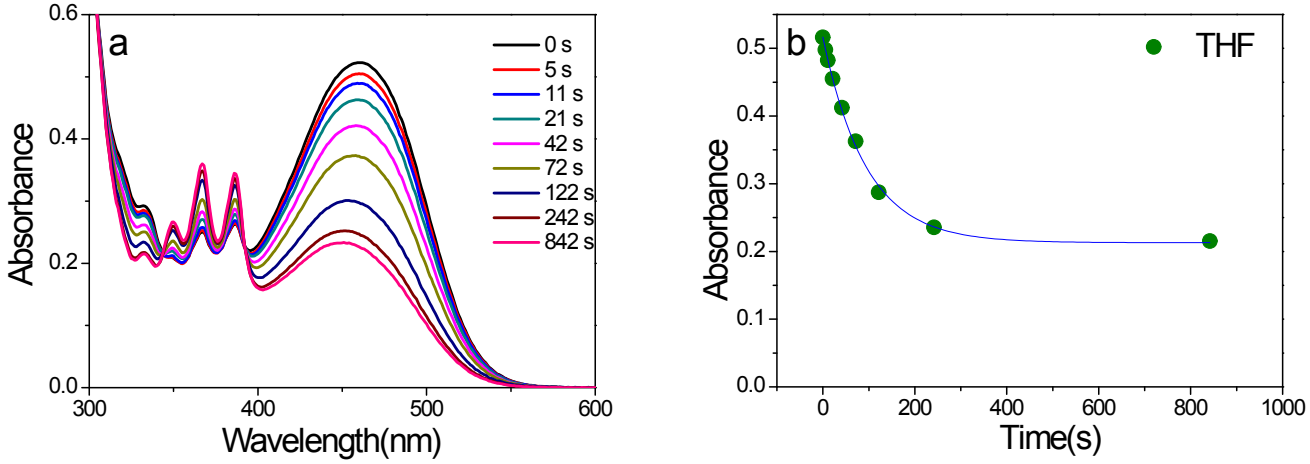

Figure S6. (a) The absorption spectrum of (E)-9DVAM in THF under 532 nm laser (Power = 1.91 mW/cm^2). Isosbestic points are at 343 nm and 392 nm. (b) The absorption of (E)-9DVAM at 462 nm in THF with the increasing of 532 nm laser irradiation. The data points are fit to the exponential in equation $A(462nm,t) = A_0 e^{-k_{abs}t} + A_{pss}$ and the analysis follows that in Hanson et al., *Photochem. Photobio. Sci.* **2015**, *14*, 1607–1616.

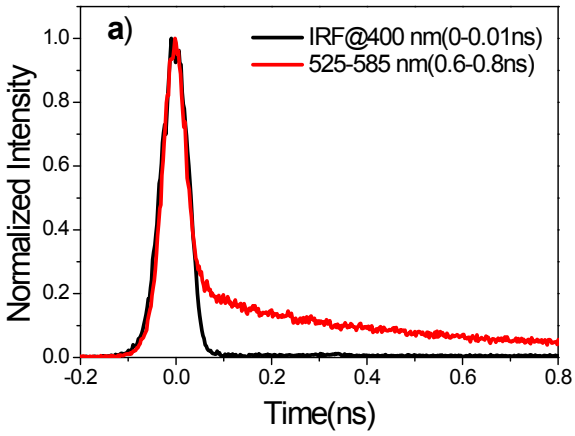

Figure S7. (a) Fluorescence lifetime data for (E)-9DVAM (red) overlaid with the instrument response function (black). 80% of the signal decays within the 30 ps time-response of the streak camera. The long-lived (~1 ns) component is due to a residual impurity centered at 450 nm that slightly overlaps the emission centered at ~550 nm. Time-resolved fluorescence lifetime data were collected using a Hamamastsu C4334 Streakscope. The E-9DVAM sample was dissolved in THF (~1.0 x 10^{-4} M). The excitation source was a 200 fs pulse centered at 400 nm, derived from frequency doubling the 800 nm output of a Coherent Libra MaiTai Ti: sapphire laser system at 1 kHz.

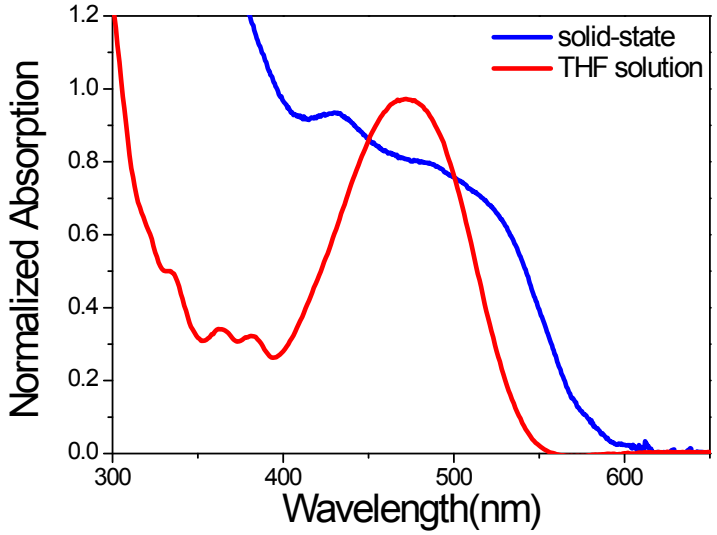

Figure S8. UV-Vis absorption spectra of (E)-9DVAM as a solid-state crystalline thin film and in solution with THF as the solvent. 1.5 mg solid of (E)-9DVAM was dissolved in 300 µL methylene chloride, then evaporated on a glass slide. During the evaporation period of solvent, 200 µL more methylene chloride was deposited onto the glass slide to get high quality solid-state thin film for UV-Vis absorption spectrum.

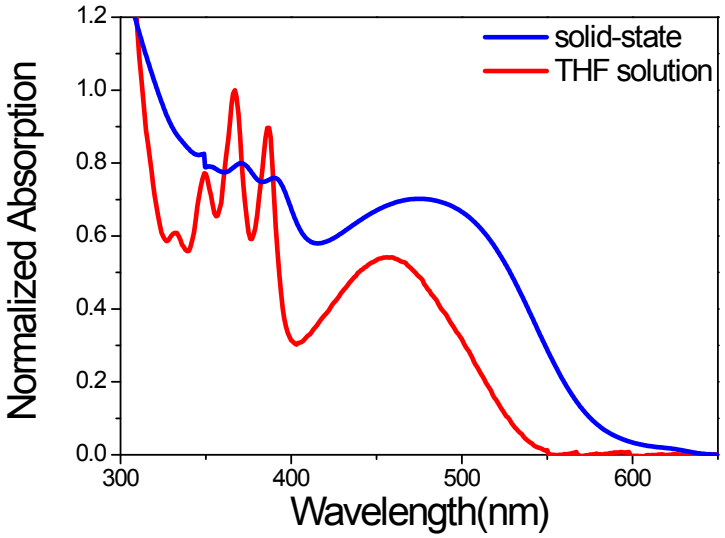

Figure S9. UV-Vis absorption spectra of (Z)-9DVAM solid-state crystalline thin film (blue line) and in solution with THF as the solvent (red line). The crystalline thin film of (Z)-9DVAM was prepared by depositing a solution of (Z)-9DVAM (1.5 mg) in 400 µL methylene chloride on a clean glass slide and allowing the solvent to slowly evaporate.

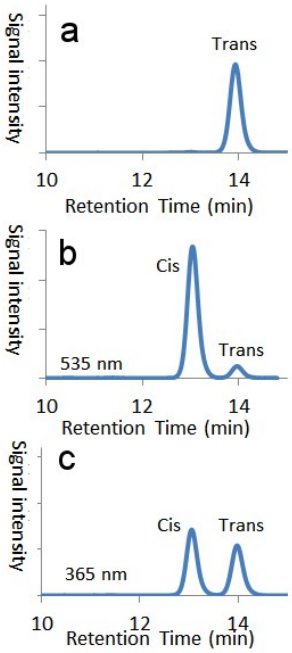

Figure S10. HPLC analysis of solution photolysis products from (E)-9DVAM: (**a**) pure (E)-9DVAM in acetonitrile (100%); (**b**) (E)-9DVAM in acetonitrile after 10 min photolysis with 535 nm (91% (Z)-9DVAM, 9% (E)-9DVAM); (**c**) Solution (b) after photolysis with 365 nm, which leads to 55% (Z)-9DVAM versus 45% (E)-9DVAM). The mobile phase was 60% CH_3CN, 40% water, pH = 2.5, Flow rate = 1.5 mL/min, Detector = 260 nm.

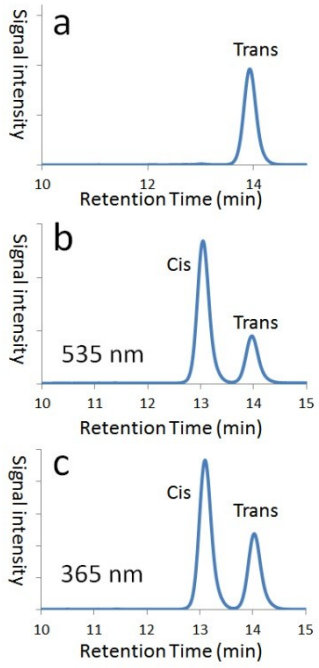

Figure S11. HPLC analysis of crystalline (E)-9DVAM photolysis products: (**a**) Pure (E)-9DVAM (100%); (**b**) (E)-9DVAM crystals after photolysis using 535 nm (75% (Z)-9DVAM, 25% (E)-9DVAM); (**c**) Sample (b) after photolysis with 365 nm (65% (Z)-9DVAM, 35% (E)-9DVAM). The mobile phase is 60% CH_3CN, 40% water, pH = 2.5, Flow rate = 1.5 mL/min, Detector = 260 nm.

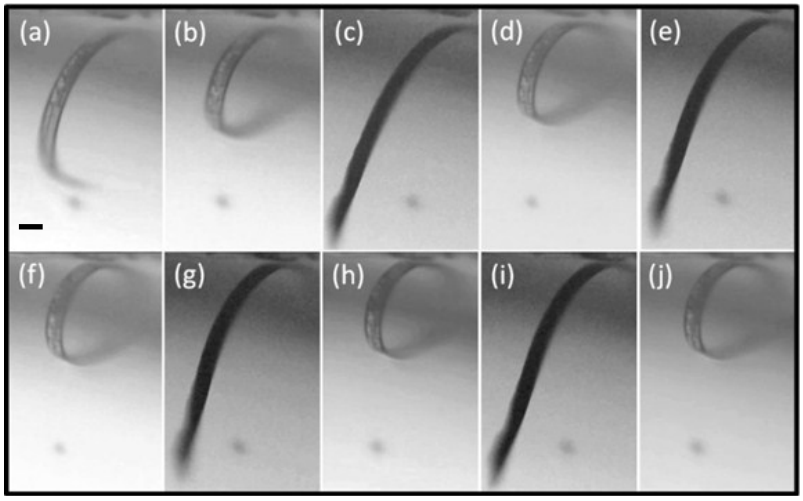

Figure S12. Sequential optical microscopy images of (**a**) Sublimed (E)-9DVAM microribbon inside of a glass tube, with one end attached to the glass tube; (**b**) after 535 nm irradiation, the ribbon bent slightly; (**c**) after 365 nm irradiation, the ribbon straightened; (**d**) after 535 nm irradiation, the ribbon bent again; (**e**) after 365 nm irradiation, the ribbon straightened; (**f**) after 535 nm irradiation, the ribbon bent; (**g**) after 365 nm irradiation, the ribbon straightened; (**h**) after 535 nm irradiation, the ribbon bent; (**i**) after 365 nm irradiation, the ribbon straightened; (**j**) after 535 nm irradiation, the ribbon bent. Scale bar = 35 μm.

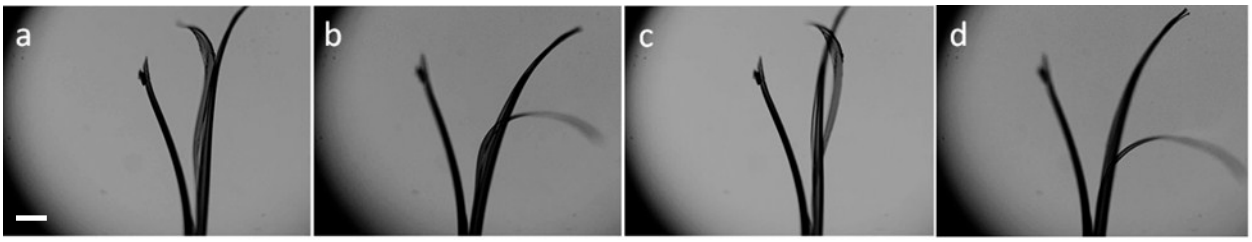

Figure S13. Optical microscopy images of a group of (E)-9DVAM microribbons actuating between UV and visible wavelength light: (**a**) before irradiation (**b**) after 535 nm light irradiation the ribbons bent away from the center; (**c**) after 365 nm irradiation the ribbons close up again ; (**d**) after 535 nm irradiation the ribbons bend away from the center. Scale bar = 120 μm.

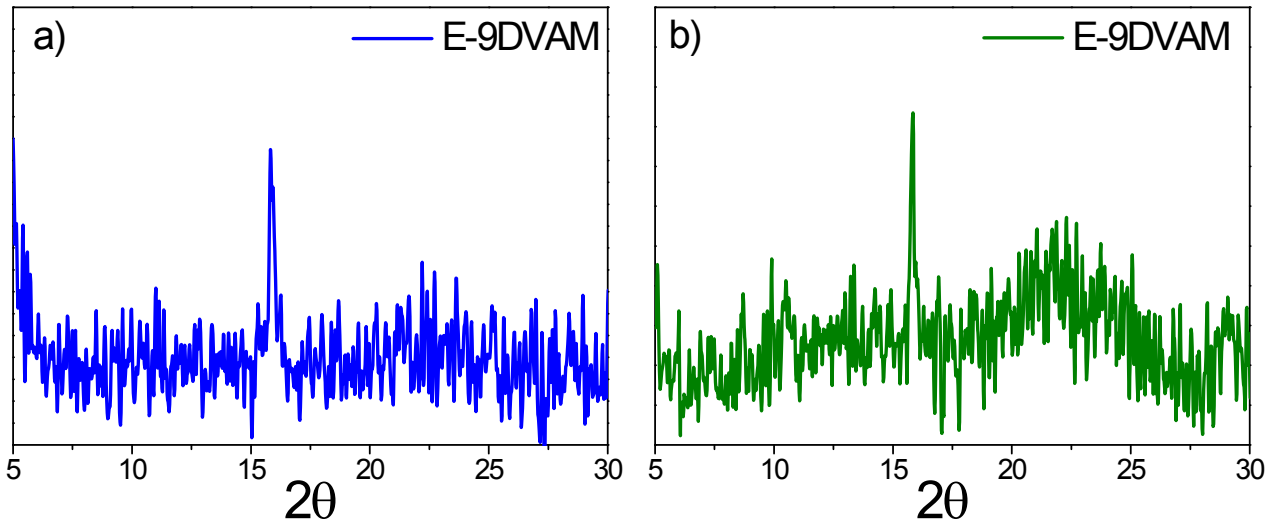

Figure S14. X-ray diffraction patterns of powders obtained by grinding up (E)-9DVAM nanowires (~200 nm in diameter) embedded in an Anodic Aluminum Oxide template (Andisc-13 from Whatman Inc). Panels (a) and (b) are two different experiments that both show the signature diffraction peak at approximately 16°, as well as weaker intensity features near 11°. Both features are also seen in the PXRD pattern of powdered crystalline (E)-9DVAM in Figure 5, confirming that the nanowires are crystalline. The broad feature between 20° and 25° is due to scattering by the amorphous alumina.